Modified Boundary Layer Resistance Model for Membrane Ultrafiltration

Tung-Wen Cheng and Jen-Guo Wu

Department of Chemical Engineering
Tamkang University
Tamsui, Taipei 251, Taiwan, R.O.C.

Abstract

The present modified boundary-layer resistance model (MBR model) includes the effect of osmotic pressure of the concentrated boundary layer on the flux. Ultrafiltration experiments were conducted in a hollow-fiber membrane module with dextran T500 aqueous solution as tested solution. The predict by the MBR model is better the osmotic pressure model or the boundary-layer resistance model and agrees pretty well with the experimental result. The over-estimation of the present model is due to the neglect of the fouling resistance.

***Key Words*:** Membrane Separation, Ultrafiltration, Boundary Layer Resistance, Osmotic Pressure

1. Introduction

Ultrafiltration has become an increasingly important separation process for the concentration, purification, or dewatering of macromolecular solutions. On an industrial scale, the following applications have been proved to be economically attractive and useful [6]: electrocoat paint recovery, latex recovery, polyvinyl alcohol recovery, oil-water separations, and miscellaneous pharmaceutical and biologic separations.

Because this process is a pressure-driven membrane separation process, the pressure applied to the working fluid provides the driving potential to force the solvent to permeate through the membrane. Typical driving pressures for ultrafiltration systems are in the range of 10 to 100 psi. For a small-applied pressure, the solvent flux through the membrane is observed to be proportional to the applied pressure. As the pressure is increased further, the flux begins to drop below that which would result from linear flux-pressure behavior. Eventually, a limiting flux is reached where the further increase in pressure will not increase the flux anymore. The flux reduction of macromolecular solution is due to the phenomena of concentration polarization, since the accumulation of retained solute on the membrane surface. Under high-pressure operation, the concentration at the membrane surface can be risen to the point of incipient gel precipitation, and a dynamic secondary membrane is formed on the top of the primary structure [1]. Because of the increased concentration, the boundary layer exerts a hydrodynamic resistance on the permeating solvent molecules [9]. Furthermore, this high concentration of macromolecule solution has an appreciable osmotic pressure [7]. The osmotic pressure of the high concentrations in ultrafiltration polarization layers can even be of the same order of magnitude as the applied pressure used in ultrafiltration [8].

The mean permeate flux of ultrafiltration is usually analyzed by using one of the following models: the gel-polarization model [5], the resistance-in-series model [10], the osmotic-pressure model [4] and the boundary-layer resistance model [9]. The integral boundary layer model [2] was also derived to predict the local permeate flux along the membrane. However, the calculation procedure of the integral boundary layer model is pretty complicated. Therefore, the models for mean permeate flux calculation are more suitable to ultrafiltraton in a practical

application. Further, the osmotic-pressure model and the boundary-layer resistance model are more theoretical meaning than the others, and they can predict the flux for a wide range of operating transmembrane pressure. In the present work, the comparison between the fluxes predicted by the osmotic-pressure model and the boundary-layer resistance model was discussed. The boundary-layer resistance model with considering the effect of osmotic pressure was also proposed. The ultrafiltration experiments were conducted in a hollow-fiber membrane module with dextran T500 aqueous solution as tested solution.

2. Theory

2.1 Water Permeability of Membrane

For the filtration of a solvent (or water), the permeate flux changes with the mean transmembrane pressure as

$$J_w = L_p \Delta P = \frac{\Delta P}{\mu_w R_m} \tag{1}$$

where J_w is the water permeate flux, ΔP, is the mean transmembrane pressure, L_p is the water permeability of the membrane, μ_w is the viscosity of water, and R_m is the intrinsic membrane resistance. The pure water permeability, L_p, or the intrinsic membrane resistance ,R_m, can be determined from the experimental data of pure water permeate flux, J_w, under various mean transmembrane pressures.

2.2 Transmembrane Pressure

In membrane ultrafiltration, the permeation rate is usually small as compared to the volumetric flow rate in the ultrafiltration membrane module. It may be assumed that the local decline in pressure within the tubular (or hollow-fiber) membrane module is simply given by the Hagen-Poiseuille equation:

$$\frac{dp(z)}{dz} = -\frac{8\mu Q_i}{N\pi r_m^4} = -\frac{8\mu u_i}{r_m^2} \tag{2}$$

where Q_i is the feed volumetric flow rate, u_i is the feed velocity, μ is the viscosity of the feed solution, r_m is the radius of the tubular (or hollow-fiber) membrane, and N is the number of tube(or fiber) in a module. Integrating Eq. (2) with the use of the boundary condition: $p = p_i$ at $z = 0$, we have the pressure distribution as

$$p(z) = p_i - mQ_i z / L = p_i - nu_i z / L \tag{3}$$

where L is the length of the membrane and

$$m = \frac{8\mu L}{N\pi r_m^4} \tag{4}$$

$$n = \frac{8\mu L}{r_m^2} \tag{5}$$

The local transmembrane pressure is obtained as the difference between the tube-side pressure and the shell-side pressure:

$$\Delta p(z) = p(z) - p_p = \Delta p_i - mQ_i z / L = \Delta p_i - nu_i z / L \tag{6}$$

where

$$\Delta p_i = p_i - p_p \tag{7}$$

The mean transmembrane pressure ΔP is obtained from following equation

$$\Delta P = \frac{1}{L}\int_0^L \Delta p(z) dz \tag{8}$$

Substitution of Eq. (6) yields

$$\Delta P = \Delta p_i - mQ_i / 2 = \Delta p_i - nu_i / 2 \tag{9}$$

2.3 Osmotic-Pressure Model (OP Model)

Kedem and Katchalsky [3] gave the following expression for the permeate flux, J_v, in ultrafiltration

$$J_v = L_p(\Delta P - \sigma \cdot \Delta\pi) \tag{10}$$

where σ and $\Delta\pi$ are the reflection coefficient and the osmotic pressure difference across the membrane, respectively. If the solute rejection is sufficiently high, σ may be assumed to be unity and the osmotic pressure difference across the membrane, $\Delta\pi$, can be found from the concentration at the membrane surface, c_m, as

$$\Delta\pi = \pi(c_m) - \pi(c_p) \cong \pi(c_m) \tag{11}$$

where the solute concentration of permeate ,c_p, is almost zero. According to Eq. (10), the effective pressure is reduced as the osmotic pressure of the retentate increases leading to a decline in the permeate flux. The osmotic pressure of a macromolecular solution can be represented as

$$\pi(c) = A_1 c + A_2 c^2 + A_3 c^3 \tag{12}$$

where A_1, A_2, and A_3 are the property constants of the macromolecular solute. Using Eqs. (11) and (12), Eq. (10) can be rewritten as

$$J_v = L_p[\Delta P - (A_1 c_m + A_2 c_m^2 + A_3 c_m^3)] \tag{13}$$

In membrane ultrafiltration, the rejected solute accumulates at the membrane surface and forms a concentration polarization layer there. At

the steady state, the quantity of the solute conveyed by the solvent to the membrane is equal to that which diffuses back. Accordingly, a material balance of the solute within the concentration boundary layer yields

$$\frac{c_m}{c_b} = \exp\frac{J_v}{k} \tag{14}$$

where c_b is the bulk solute concentration in the retentate, and k is the mass transfer coefficient. In ultrafiltration systems, the bulk concentration of the retentate, c_b, may be considered to be equal to the feed concentration c_i. As L_p and k are known, the value of J_v and c_m can be determined from solving Eqs. (13) and (14).

The mass transfer coefficient k in the concentration polarization layer can be determined from the Leveque equation if the flow in the module is laminar

$$k = 1.62\left(\frac{u_i D^2}{2 r_m L}\right)^{1/3} \tag{15}$$

where D is the solute diffusivity in the solvent.

2.4 Modified Boundary-Layer Resistance Model (MBR Model)

The boundary layer in ultrafiltration can be seen as a stagnant, concentrated polymer solution through which the solvent permeates. Wijmans et al. [9] proposed the conventional boundary-layer resistance model (BR model) for the flux calculation in ultrafiltration as

$$J_v = \frac{1}{\mu_w}\frac{\Delta P}{R_m + R_{bl}} \tag{16}$$

where R_{bl} is the hydrodynamic resistance of the concentration boundary layer. A modified model which considering both effects of osmotic pressure and the boundary layer resistance on flux was proposed in the present work as

$$J_v = \frac{1}{\mu_w}\frac{\Delta P - \Delta\pi(c_m)}{R_m + R_{bl}} \tag{17}$$

The resistance of the concentration boundary layer is defined as

$$R_{bl} = \int_0^{\delta}\frac{1}{L_{bl}(y)}dy \tag{18}$$

where L_{bl} is the permeability of solute through the boundary layer and δ is the thickness of the boundary layer. The relation between the solvent permeability and the solute sedimentation in the boundary layer can be expressed as

$$L_{bl}(y) = \frac{\mu_w s}{(1 - V_s/V_w)\, c} \tag{19}$$

where s is the sedimentation coefficient of the macromolecule solute, V_s and V_w are the partial molar volumes of solute and solvent, respectively. The concentration dependence of the sedimentation coefficient is usually expressed as

$$\frac{1}{s} = \frac{1}{s_0}\left(1 + K_1 c + K_2 c^2\right) \tag{20}$$

The coefficients K_1 and K_2 are constant for the macromolecule solute.

The concentration of the solute in the boundary layer is the function of the distance from the membrane surface. Mass balance of the solute in the boundary layer yields

$$J_v\, c = D\frac{dc}{dy} \tag{21}$$

or

$$c = c_i\, exp\frac{J_v y}{D} \tag{22}$$

Substituting Eqs. (19), (20) and (22) into Eq. (18), one obtains the boundary layer resistance as

$$R_{bl} = \frac{(1 - V_s/V_w)D}{\mu_w s_0 J_v}[(c_m - c_i) + \frac{K_1}{2}(c_m{}^2 - c_i{}^2) + \frac{K_2}{3}(c_m{}^3 - c_i{}^3)] \tag{23}$$

Therefore, the predicted flux will be also obtained from boundary-layer resistance model, Eq. (16), or the modified boundary-layer resistance model, Eq. (17) combining with Eqs. (14) and (23).

3. Experiment

The experimental apparatus used in this work is shown in Figure 1. The Amicon H1P30-20 hollow-fiber cartridges ($r_m = 2.5\times10^{-4}$ m, L = 0.153 m, and effective membrane area = 600 cm^2) were employed for ultrafiltration of aqueous solution of Dextran T500. The tested solute was dextran T500 (Pharmacia Co., Sweden) which was more than 99% retained by the membrane used. The solvent was distilled water.

The feed solution was circulated by a high-pressure pump with a variable speed motor (L-07553-20, Cole-Parmer Co.); the liquid flow rate

was observed by a flowmeter (IR-OPFLOW 502-111, Headland Co.). The feed pressure was controlled by using an adjustable valve at the outlet of the membrane module, and the gauge pressures at the tube-side inlet (p_i), outlet (p_o) and at the shell-side (p_p) were measured with a pressure transmitter (Model 891.14.425, Wika Co.).

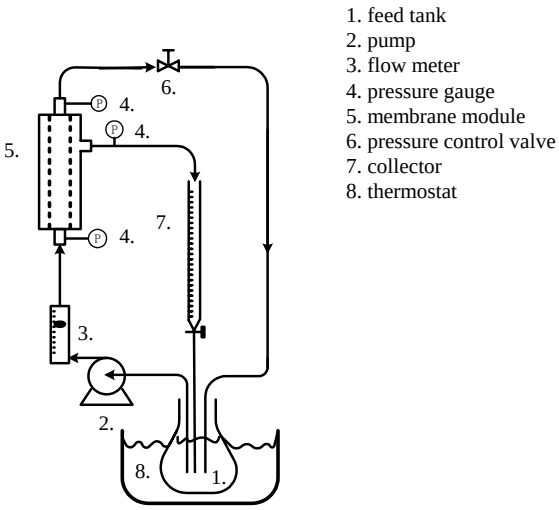

Figure 1. Flow diagram of ultrafiltration appartus.

The ranges of the experimental conditions were as follows. The feed concentration, c_i, were 2.0-16.0 g/l; the feed velocity, u_i, were 0.10-0.30 m/s; and the feed transmembrane pressures, Δp_i, were 58.8-156.8 kPa. The feed solution temperature in all experiments was kept at 30 ^{o}C by a thermostat. During each run, both the permeate and the retentate were recycled back to the feed tank. After each experiment, the membrane was cleaned by high circulation and backflushing with 0.1N NaOH aqueous solution and pure water. The cleaning procedure was repeated until the original water flux had been restored.

The physical properties of dextran T500 aqueous solution can be estimated as follows:

The diffusivity [9]

$$D(c)\times 10^{11} = 1.204 + 2.614\times 10^{-2} c - 4.167\times 10^{-5} c^2 + 2.132\times 10^{-8} c^3 \quad \left(m^2 \cdot s^{-1}\right) \tag{24}$$

The osmotic pressure [7]

$$\pi(c) = 6.55c + 1.038c^2 + 0.00753c^3 (Pa) \tag{25}$$

The viscosity

$$\mu = 0.8937\times 10^{-3} \exp(0.0371 c_i) \quad (Pa \cdot s) \tag{26}$$

The sedimentation coefficient [9]

$$\frac{1}{s} = \frac{1}{8.5\times 10^{-13}} \left(1 + 106 \cdot c + 617 \cdot c^2\right) \quad \left(s^{-1}\right) \tag{27}$$

The unit of concentration in above equations is in g/l. The partial volume of dextran T500 is 0.644×10^{-3} m^3/kg.

4. Results and Discussion

4.1 Determination of Water Permeability

Figure 2 is the plot of pure water ultrafiltrated flux under various transmembrane pressures. The relationship between $1/J_w$ and $1/\Delta P$ is nearly a straight line. From the slope of the least square line, obtains the water permeability of the membrane is 4.72x10^{-10} m^{3}Ps^{-1}m^{-2}s^{-1}.

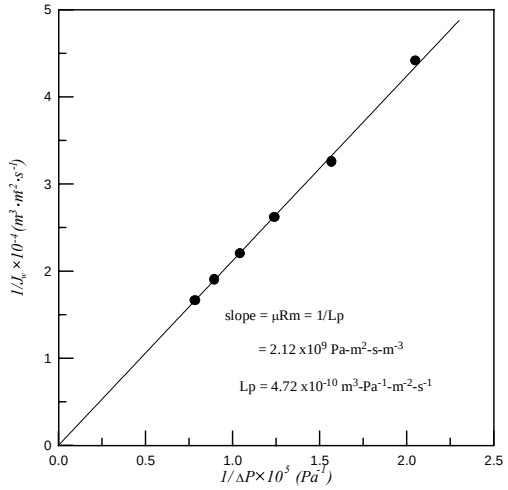

Figure 2. Permeate flux of pure water.

4.2 Predicted Fluxes of various Models

Figure 3 is the plots of experimental data and the predicted fluxes by osmotic pressure model. The feed concentration was 2.0 g/l and the liquid velocity varied from 0.1 to 0.3 m/s. Experimental data increase with the transmembrane pressure and the liquid velocity. The predicted flux has same tendency as the experimental data, however, predicts are larger than the experimental data.

The prediction by the boundary-layer resistance model was shown Figure 4. Those predicts are larger than the experimental data and further higher than the predicts by the osmotic pressure model.

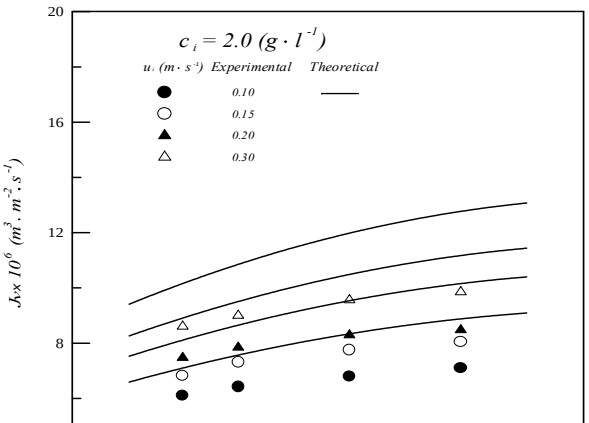

Figure 3. Flux predicted by osmotic pressure model (c_i = 2.0 g/l).

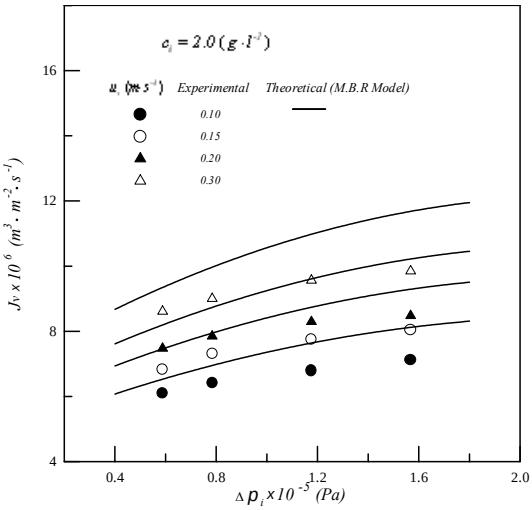

Figure 4. Flux predicted by boundary-layer resistance model (c_i = 2.0 g/l).

Taking account of the osmotic pressure and the boundary-layer resistance, the MBR model agrees pretty well with the experimental data, as shown in Figure 5. The prediction is still higher than the experimental data, however, the MBR model gives a better prediction than the other two.

4.3 Comparison between the Experimental Data and Predicts of MBR Model

Figures 6, 7 and 8, respectively, are the plots of the experimental data and predicts by the modified boundary-layer resistance model for 4.0, 8.0 and 16.0 g/l feed concentration. The result shows that predicts are higher than the experimental data, especially for a concentrated feed solution. The over-estimation is due to the neglect of solute fouling phenomenon in

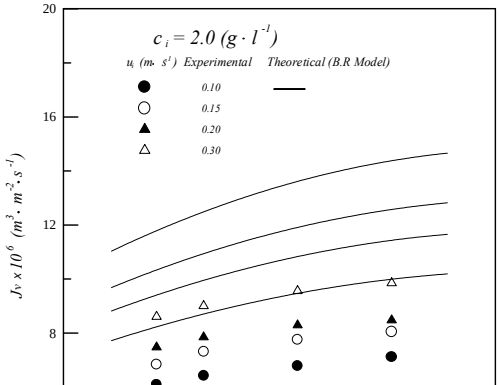

Figure 5. Flux predicted by MBR model (c_i = 2.0 g/l).

the theoretical model. The adsorption or fouling of solute on the membrane structure will increase the filtration resistance. The present model does not include the term of fouling resistance, so the predict is higher than the experimental data. The more concentrated the feed solution, the larger the fouling resistance. Therefore, the deviation of the predict from the experimental data is wide for the concentrated feed.

5. Conclusion

Comparison of the fluxes calculated by the osmotic-pressure model, the boundary-layer resistance model as well as the modified boundary-layer resistance model was discussed in this work. The modified boundary-layer resistance model (MBR model) includes the effect of osmotic pressure of the concentrated boundary layer on the flux. The ultrafiltration experiments were conducted in a hollow-fiber membrane module with dextran T500 aqueous solution as tested solution. The predict by the MBR model is better the other two models and agrees pretty well with the experimental data. The prediction is higher than the experimental data, however. The over-estimation in flux by the present model is due to the neglect of the fouling resistance, which is significant for the concentrated macromolecular solution on the hollow-fiber membrane.

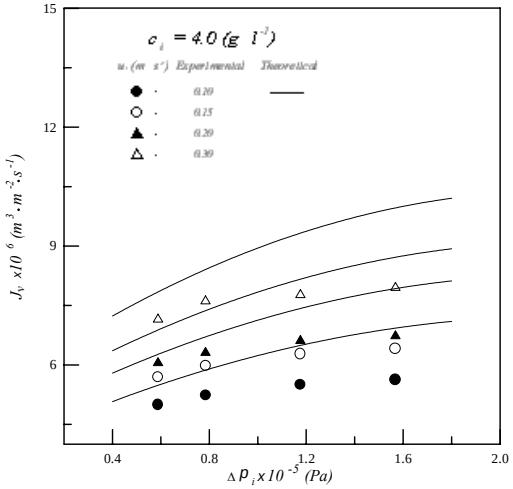

Figure 6. Flux predicted by MBR model (c_i = 4.0 g/l)
.

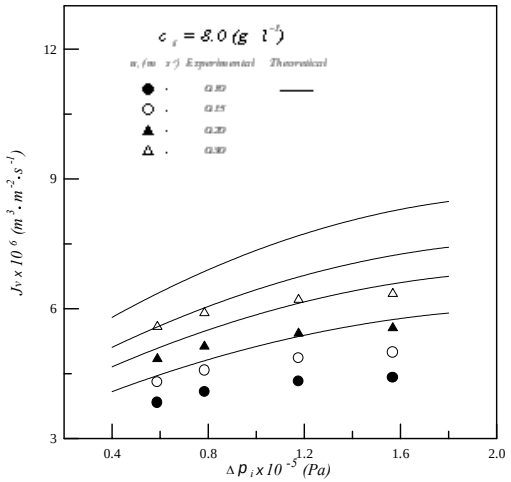

Figure 7. Flux predicted by MBR model (c_i = 8.0 g/l).

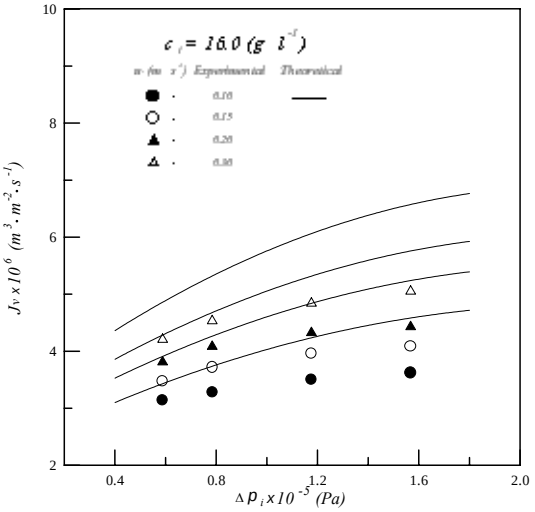

Figure 8. Flux predicted by MBR model (c_i = 16.0 g/l).

Acknowledgment

The authors wish to express their thanks to the Nation Science Council, R.O.C., for the financial aid.

Nomenclature

A_1, A_2, A_3	constant defined in Eq. (12)
c_b	solute concentration in bulk retentate (g/l)
c_m	solute concentration on membrane surface (g/l)
D	diffusion coefficient (m^2/s)
J_v	permeate flux of solution ($m^3m^{-2}s^{-1}$)
J_w	permeate flux of pure water ($m^3m^{-2}s^{-1}$)
k	mass transfer coefficient (ms^{-1})
L	length of tubular membrane (m)
L_{bl}	solvent permeability in solute (m^2)
L_p	pure water permeability ($m^3Pa^{-1}m^{-2}s^{-1}$)
p	pressure of tube-side (Pa)
p_i	inlet pressure of the tube-side (Pa)
p_p	pressure of permeate phase (Pa)
Δp	transmembrane pressure (Pa)
ΔP	mean transmembrane pressure (Pa)
Q	volume flow rate (m^3/s)
r_m	radius of hollow fiber (m)
R_m	resistance of membrane (m^{-1})
R_{bl}	resistance of boundary layer (m^{-1})
s	sedimentation coefficient of solute (sec)
s_0	s at infinite dilution (sec)
u_i	feed velocity (ms^{-1})
V_s	partial specific volume of solute (ml/g)
V_w	partial specific volume of water (ml/g)
z	axial coordinate (m)

Greek letters

δ	thickness of boundary layer (m)
σ	reflection coefficient
μ	viscosity of solution (Pa-s)
μ_w	viscosity of pure water (Pa-s)
π	osmotic pressure (Pa)
$\Delta\pi$	osmotic pressure difference (Pa)

References

[1] Blatt, W. F., Dravid, A., Michael, A. S. and Nelsen, L., "Solute Polarization and Cake Formation in Membrane Ultrafiltration: Causes, Consequences, and Control Techniques," *Membrane Science and Technology*, J. E. Flinn, ed., Plenum Press, New York, pp. 47-97, (1970).

[2] Cheng, T. W., Yeh, H. M. and Wu, J. G., "Permeate Flux Prediction by Integral Osmotic-Pressure Model for Ultrafiltration of Macromolecular Solutions," *J. Chin. I. Chem. Engrs.* 29, 193 (1998).

[3] Kedem, O. and Katchalsky, A., "A Physical Interpretation of the Phenomenological Coefficients of membrane Permeability," *J. Gen. Physiol*., 45, 143 (1961).

[4] Nabetani, H., Nakajima, M., Watanabe, Nakao, A., S. and Kimura, S., "Effects of Osmotic Pressure and Adsorption on Ultrafiltration of Ovalbumin," *AIChE J*., 36, 907 (1990).

[5] Porter, M.C., "Concentration Polarization with Membrane Ultrafiltration," *Ind. Eng. Chem. Prod. Res. Develop.*, 11, 234 (1972).

[6] Porter, M. C., "Membrane Filtration," In *Handbook of Separation Techniques for Chemical Engineers*. (P. A. Schweizter, Ed.), McGraw-Hill, New York (1979).
[7] Vink, H., "Precision Measurements of Osmotic Pressure in Concentrated Polymer Solutions," *Eur. Polym. J.*, 7, 1411 (1971).
[8] Wijmans, J. G., Nakao, S. and Smolders, C. A., "Flux Limitation in Ultrafiltration: Osmotic Pressure Model and Gel Layer Model," *J. Membrane Sci.*, 20, 115 (1984).
[9] Wijmans, J. G., Nakao, S., Van Den Berg, J. W. A., Troelstra, F. R. and Smolders, C. A., "Hydrodynamic Resistance of Concentration Polarization Boundary Layers in Ultrafiltration," *J. Membrane Sci.*, 22, 117 (1985).
[10] Yeh, H. M. and Cheng, T. W., "Resistance-in-Series for Membrane Ultrafiltration in Hollow Fibers of Tube-and-Shell Arrangement," *Sep. Sci. Technol.*, 28, 1341 (1993).

Accepted: Jun. 22, 2001